

Microscopic Imaging and Labeling Dataset for the Detection of *Pneumocystis jirovecii* Using Methenamine Silver Staining Method

Erick Reyes-Vera ^{1,2,*}, Juan S. Botero-Valencia ^{3,†}, Karen Arango-Bustamante ², Alejandra Zuluaga ² and Tonny W. Naranjo ^{2,4}

¹ Department of Electronics and Telecommunications, Instituto Tecnológico Metropolitano ITM, Medellín 050034, Colombia

² Medical and Experimental Mycology Group, Corporación para Investigaciones Biológicas, Medellín 050034, Colombia; karango@cib.org.co (K.A.-B.); azuluaga@cib.org.co (A.Z.); tonny.naranjo@upb.edu.co (T.W.N.)

³ Department of Mechatronics and Electromechanics, Instituto Tecnológico Metropolitano ITM, Medellín 050034, Colombia; juanbotero@itm.edu.co

⁴ School of Health Sciences, Universidad Pontificia Bolivariana, Medellín 050031, Colombia

* Correspondence: erickreyes@itm.edu.co

† These authors contributed equally to this work.

Abstract: *Pneumocystis jirovecii* pneumonia is one of the diseases that most affects immunocompromised patients today, and under certain circumstances, it can be fatal. On the other hand, more and more automatic tools based on artificial intelligence are required every day to help diagnose diseases and thus optimize the resources of the healthcare system. It is therefore important to develop techniques and mechanisms that enable early diagnosis. One of the most widely used techniques in diagnostic laboratories for the detection of its etiological agent, *Pneumocystis jirovecii*, is optical microscopy. Therefore, an image dataset of 29 different patients is presented in this work, which can be used to detect whether a patient is positive or negative for this fungi. These images were taken in at least four random positions on the specimen holder. The dataset consists of a total of 137 RGB images. Likewise, it contains realistic, annotated, and high-quality microscope images. In addition, we provide image segmentation and labeling that can also be used in numerous studies based on artificial intelligence implementation. The labeling was also validated by an expert, allowing it to be used as a reference in the training of automatic algorithms with supervised learning methods and thus to develop diagnostic assistance systems. Therefore, the dataset will open new opportunities for researchers working in image segmentation, detection, and classification problems related to *Pneumocystis jirovecii* pneumonia diagnosis.

Dataset: <https://doi.org/10.17605/OSF.IO/WQME8>.

Dataset License: CC-BY Attribution 4.0 International.

Keywords: *Pneumocystis jirovecii* pneumonia; Grocott's methenamine silver; microscopy; diagnosis; labeling; digital image processing; non-destructive tests



Citation: Reyes-Vera, E.; Botero-Valencia, J.S.; Arango-Bustamante, K.; Zuluaga, A.; Naranjo, T.W. Microscopic Imaging and Labeling Dataset for the Detection of *Pneumocystis jirovecii* Using Methenamine Silver Staining Method. *Data* **2022**, *7*, 56. <https://doi.org/10.3390/data7050056>

Academic Editor: Li-Yueh Hsu

Received: 16 February 2022

Accepted: 15 April 2022

Published: 29 April 2022

Publisher's Note: MDPI stays neutral with regard to jurisdictional claims in published maps and institutional affiliations.



Copyright: © 2022 by the authors. Licensee MDPI, Basel, Switzerland. This article is an open access article distributed under the terms and conditions of the Creative Commons Attribution (CC BY) license (<https://creativecommons.org/licenses/by/4.0/>).

1. Summary

Pneumonia is a common respiratory infection that primarily affects the alveoli and the distal bronchial tree of the lungs. It is an infection caused by viruses, bacteria, fungi, or other germs that causes inflammation of one or both lungs and can be treated if detected early [1–3]. In the case of pneumonia caused by fungus, the principal etiological agent is an opportunistic fungal pathogen called *Pneumocystis jirovecii*. *Pneumocystis jirovecii* pneumonia (PCP) is an opportunistic fungal infection that is potentially fatal, especially

in children and the elderly; PCP most commonly affects human immunodeficiency virus (HIV)-infected individuals, chemotherapy recipients, malnourished children, and organ transplant patients [4,5]. In fact, at least 95% of the world's population is thought to have been infected with this fungus in childhood, but adults are asymptomatic carriers of this infection [4]. For this reason, diagnostic techniques and tools are needed to detect infection with this fungal pathogen in a timely manner, as this could help save the lives of more people [4,6]. In addition, there is a need to increase the sensitivity of current diagnostic tests. Examples can be seen where artificial intelligence is used on chest X-ray images to diagnose pneumonia [7,8] and symptoms [9] and to assess severity [10]; however, new techniques based on bronchial lavage, bronchoalveolar lavage, sputum, or tracheal aspirates have not been widely explored.

Currently, several techniques are used to diagnose *Pneumocystis jirovecii* pneumonia. The most commonly used techniques and tools worldwide include optical microscopy [1,6,11–13], fluorescence microscopy [6], polymerase chain reaction (PCR) [3,12,14], and chest X-ray [2,15]. Fluorescence-microscopy-based techniques are quite good for detecting PCP. However, this technique requires reagents that are sometimes expensive, such as calcofluor white [6]. In addition, fluorescence microscopes are more expensive than light microscopes, making them inaccessible to some diagnostic centers and hospitals, especially in regions far from large cities. On the other hand, polymerase chain reaction (PCR) is a more sensitive technique; however, this technique is usually more expensive and is not available in all emergency rooms, villages, or outpatient settings [6]. Moreover, this technique requires an expert in molecular methods to be implemented. In the same way, the chest-X-ray-based technique requires specialized equipment, which means that it cannot be used everywhere. In addition, this method also requires expert personnel, a large space where the equipment can be installed, and the adequacy of the installations. Optical microscopy examinations usually have limitations compared to other techniques such as PCR, which are related to the expertise of the personnel in charge of performing the microscopic evaluation. Moreover, in many cases, although the clinical samples are always prepared according to the same protocol, the stain results are variable depending on different factors related to the patient and clinical sample. This means that the sensitivity of microscopic techniques ranges from 55% to 78% [6,12]. Therefore, it is necessary to integrate modern technologies such as digital imaging, artificial intelligence, and computer vision, among others, to improve the sensitivity and reduce the frequency of false-positive or -negative diagnoses. This will eliminate, in some cases, the dependence on the expert for a rapid diagnosis and improve the detection of this infection in diagnostic centers, hospitals, and laboratories.

In recent years, research has intensified in the field of computer techniques and devices to enhance and extract more information from images [16–23]. In these reports, there has been a pronounced interest in the use of artificial-intelligence-based techniques to automatically diagnose disease, infection, imperfections, or any sign of change compared to a normal scenario. For example, in 2013, Vakilian et al. reported an artificial neural network (ANN) for identifying fungal diseases on cucumber plants using digital image processing [18]. This method allows the identification of two fungi species (*Pseudoperonospora cubensis* and *Sphaerotheca fuliginea*) in cucumber plants. Likewise, it helps to better predict the hours after incubation of an infected leaf. Mader et al. used fluorescence microscopy to detect fungal infections of the skin [21]. They also improved the quality of diagnosis by using an image processing scheme. In this scheme, the microscopic images were pre-processed, segmented, parameterized, and classified to automate the detection of such infections. In the same way, Pujari et al. employed image processing techniques for the detection of fungal diseases in vegetable, cereal, fruit, and commercial crops [24]. Likewise, an automatic diagnosis of vulvovaginal candidiasis (VVC) from Pap smear images was reported by Momenzadeh et al. [17]. The authors developed an artificial vision-based algorithm that can distinguish *Candida* (pseudo) hyphae and blastospores. The algorithm enables automatic detection of VCC from microscope images and also helps in identifying features such as shape, size, and color. In recent reports, some researchers have developed a technique to

detect pneumonia in patients using digital imaging. However, in this case, the analysis is performed using chest radiographs. For example, in 2019, Saraiva et al. presented a comparison between two neural networks for pneumonia detection and classification [2]. Two deep learning techniques known as convolutional neural networks (CNNs) and Multilayer perceptron (MLP) were used for classification. They showed that CNN technique has higher accuracy in these types of experiments. Similarly, Jaiswal et al. applied a deep learning approach to detect pneumonia in chest X-rays [15]. However, they implemented a Mask regression-CNN-based methodology, which involves some modifications in the segmentation step. On the other hand, Sirazitdinov et al. proposed a computational method based on the combination of two CNNs, namely RetinaNet and Mask regression CNN, to detect and localized pneumonia [22]. Most recently, an image processing technique for automatic detection of COVID-19 using X-ray and computed tomography images was presented by Kassani et al. In this case, several machine learning algorithms were trained to extract features from the images [23].

To date, there is no database in which the diagnosis of *Pneumocystis jirovecii* pneumonia is made on the basis of images taken with a light microscope. Therefore, we believe that the proposed database can help improve the diagnosis of this disease, which affects a large number of people around the world every year. These data can be used for the training, testing, and validation of different computational models related to object detection, image segmentation techniques, and medical diagnosis based on image processing. In addition, the reported dataset can be useful for researchers working in computer-vision-based models due to these images and their respective segmentation being able to be used to perform image classification and *Pneumocystis jirovecii* pneumonia detection using artificial-intelligence-based algorithms. This type of data is essential for training artificial intelligence techniques by supervised methods and for developing applications to assist in medical diagnostics [25,26]. Finally, the expert annotations can be used to develop and improve the diagnosis of *Pneumocystis jirovecii* in clinical patients using statistical analysis.

2. Materials and Methods

In this section, the methods used for sample preparation, image acquisition, and its processing are explained in detail. Likewise, the materials and equipment necessary to carry out the experiments are presented. Thus, Section 2.1 presents the materials used and their respective quantities. Section 2.2 details the procedure followed for the preparation of laboratory samples. The protocol employed, the characteristics of the collected images, and the details of how the images were acquired are presented in Section 2.3. Finally, image processing and segmentation are explained in detail in Section 2.4.

2.1. Materials

The following materials and reagents were used to carry out the experiment [27,28]: isopropyl alcohol, 5% periodic acid, 1% sodium bisulfite, 3% methenamine, 5% silver nitrate, 5% Borax, 0.1% gold chloride, 2% sodium thiosulfate, 0.1% toluidine blue, N-acetyl cysteine, 2.94% sodium citrate, Entellan UN 1866 Merck, and glass slides. In addition, it was necessary to use the following laboratory equipment: stove, biosecurity camera, centrifuge, Leica ICC50 HD camera, and Leica DM500 microscope.

2.2. Samples' Preparation

Grocott's methenamine silver is the most commonly used staining method for fungal diagnosis [27–30]. When performing methenamine silver staining, special care must be taken with all procedures such as reagent preparation and reaction times, as this can adversely affect the quality of the stain and, thus, the diagnosis. The first step was to process the samples, which should be performed in a biological safety cabinet. For respiratory samples (bronchial lavage, bronchoalveolar lavage, sputum, tracheal aspirates), it is important to first centrifuge them at 3000 rpm for 30 min at a temperature of 4 °C. The supernatant was then discarded, the sediment was vortexed, and a drop of the sample was placed

on a slide using a Pasteur pipette, spread and dried in the chamber. For tissue samples, the tissue must be cut into small fragments using a scalpel, pestle, and mortar. Furthermore, the sample must be hydrated with sterile saline. Then, a drop of this material was placed on a slide with a Pasteur pipette, spread and dried in the biosafety chamber. Once the microscope slide samples were dry, they were placed in a glass Coplin box, which was the container where the staining process was carried out.

The microscope slide samples were first fixed with 100 mL of isopropyl alcohol for 30 min, then the alcohol was removed, and distilled water was added to hydrate the samples for 30 min. After that, the water was discarded, and 100 mL of 5% periodic acid was added for one hour. Subsequently, this reagent was removed and washed with tap water several times (approximately 3 times), 100 mL of 1% sodium bisulfite was added for 1 min, the reagent was removed, and another 100 mL of tap water was added for 5 min, then discarded and washed again with sterile water. The stock solution (50 mL of 3% methenamine and 2.5 mL of 5% silver nitrate) and the working solution (50 mL of stock solution, 50 mL of distilled water, 4 mL of 5% borax) were prepared. The working solution was added to the Coplin box containing the microscope slide samples and incubated at a temperature equal to 70 °C for approximately 1 h or until the sample turned a tamarind color.

The microscope slide samples should be placed in another Coplin box with 100 mL of distilled water, which should be at the same temperature of 70 °C. When all the microscope slide samples take the expected color, they should be washed again with distilled water for 2 min, then discarded, and 100 mL of 0.1% Gold Chloride was added until the samples took a grey color (approximately 1 min). Then, the Gold Chloride was removed, the microscope slide samples were washed with distilled water, and 100 mL of 2% sodium thiosulphate was added for 3 min. After, the sodium thiosulfite was removed, they were washed with distilled water, and 100 mL of 0.1% toluidine blue was added for 3 min. Finally, the toluidine blue was removed, they were washed again with distilled water, and the microscope slide samples were placed on a tray to dry. When the microscope slide samples were dry, a glass slide with Entellan was mounted on the plate to fix it for observation under the optical microscope.

2.3. Image Acquisition

To capture the image of the samples under test, a Leica DM500 microscope using a Leica ICC50 High Definition (HD) camera (Leica Microsystems, Wetzlar, Germany) was employed. The Leica LM500 is a microscope commonly utilized in the diagnostic unit of the Corporación para Investigaciones Biológicas (CIB) (Medellín, Colombia). Moreover, the camera of this optical microscope has a sensor size of 6.55 mm × 4.92 mm (pixel size 3.2 µm × 3.2 µm). In our case, each image was captured using a magnification of 40× (Numerical Aperture (NA) equal to 0.65), while the glass slide was illuminated with a light-emitting diode (LED) source. Likewise, lighting and contrast were kept constant in the analysis of all samples to ensure good homogeneity of the images. To ensure a database with an adequate size, samples from 29 different patients were analyzed using the optical microscope. In addition, the image acquisition was taken in at least four different positions on the glass slide, as depicted in Figure 1. These positions were randomly selected over the area where the sample was located with *Pneumocystis jirovecii*. Thus, we obtained a dataset with 137 RGB images, which had a resolution of 2048 × 1536 with 24 bit color intensity in every pixel.

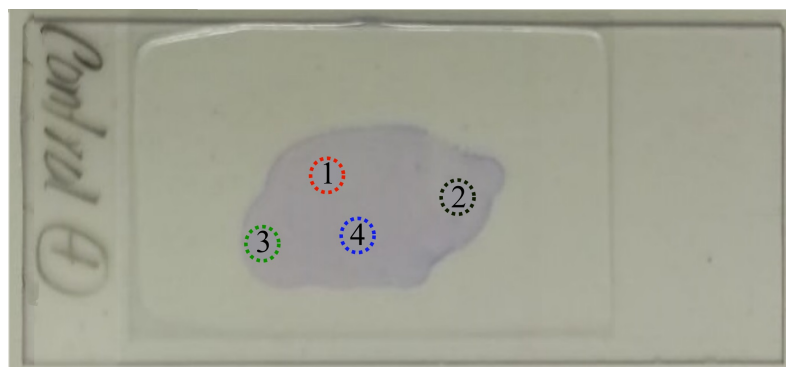


Figure 1. Photograph of the analyzed glass slides. The circles with a dotted line mark random positions on the sample.

2.4. Image Processing

The labeling process consisted of developing an artificial mask image, which allows identifying the elements in the analysis image. In this case, it was decided to mark the three areas with larger objects using red, green, and blue labels. The processing started with an automatic contrast adjustment to improve definition, thresholding (conversion to black and white), then a morphological opening operation to smooth and eliminate small elements, then a segmentation to identify the connected objects, then the three elements with the largest area were selected, and finally, these were labeled to generate the artificial image that could be used as a reference. After being labeled, an expert on the observation and identification of *Pneumocystis jirovecii* reviewed and built the identification file for the presence of *Pneumocystis jirovecii* on the samples under test. Figure 2 shows the sequence of the process.

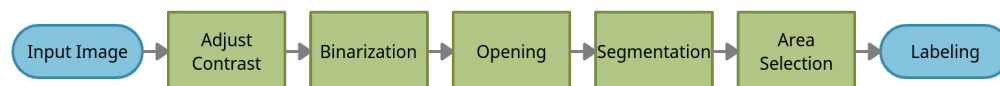


Figure 2. Summary of the image labeling process.

3. Data Description

This dataset consisted of a set of images obtained using the method described in Section 2.3. An example of the microscopy image and the labeled image are illustrated in Figure 3a and Figure 3b, respectively. As mentioned earlier, the database presented in this work contained a total of 137 RGB images that can be used for the diagnosis of *Pneumocystis jirovecii* pneumonia. The path to access the collected images is shown in Figure 4, where the structure inside the repository, the version of each image, and the date can be seen, and in the root is the file “Labels.xlsx” with the labels of all the data and, inside each folder, the corresponding images. Likewise, The database can be accessed through the following link: <https://doi.org/10.17605/OSF.IO/WQME8>, accessed on 15 February 2022) (remember that samples from 29 different patients were analyzed). In turn, each folder contains photographs in at least four different positions to ensure correct diagnosis, as shown previously in Figure 1. To distinguish the images, a label was created according to the following nomenclature: MuestraXX_PosYYY.JPG, where XX and YY denote the sample analyzed and the position on the slide. For example, it is possible to find the image named Muestra1_Pos1.JPG inside the folder Sample01 (see Figure 3a). On the other hand, each folder also contains the labeled image (the segmentation was already described in Section 2.4). To distinguish it from the original image taken with the microscope, _L was added after the image name, for example: Muestra1_Pos1_L.JPG. These can be used directly in the classification and analysis algorithms of diagnostic images; in Figure 3b, the corresponding labeled image can be seen.

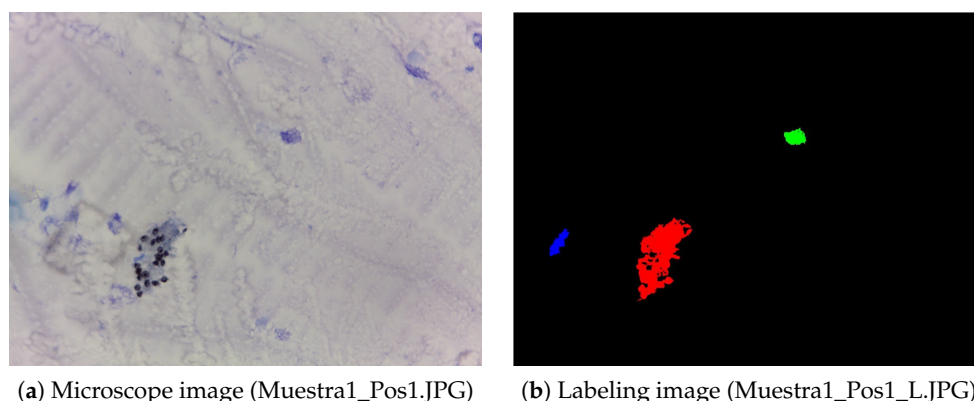


Figure 3. Example of acquired and labeled image are illustrated. (a) Optical image obtained with the Leica DM500 microscope using a magnification of 40×. (b) Segmented image used in the labeled process.

Finally, the labeling of all images was performed with the help of an expert (K. Arango). The file Labels.xlsx contains the labels for each segment of the image. These labels allow using this database in different studies related to artificial intelligence and classification techniques of image processing. The labeled images are an artificial version where the RGB channel is used to create a mask that facilitates (at the programming level) the location of artifacts in the image; in this case, for each channel, one will find “1” on the first object found in the image in the R channel and 0 for the rest of the image, and for the G channel, one will find with “1” the second object and for the B channel the third.

Name	Size	Version	Downloads	Modified
Microscopic imaging and labeling dataset for the detection of <i>Pneumocystis jirovecii</i> using methenamine silver stain...				
OSF Storage (United States)				
Labels.xlsx	50.9 kB	1	0	2021-12-16 10:14 AM
Sample01				
Muestra1_Pos1.JPG	1.3 MB	1	0	2021-11-27 11:19 PM
Muestra1_Pos1_L.JPG	33.5 kB	1	0	2021-11-27 11:19 PM
Muestra1_Pos2.JPG	1.3 MB	1	0	2021-11-27 11:19 PM
Muestra1_Pos2_L.JPG	48.7 kB	1	0	2021-11-27 11:19 PM
Muestra1_Pos3.JPG	1.3 MB	1	0	2021-11-27 11:19 PM
Muestra1_Pos3_L.JPG	53.2 kB	1	0	2021-11-27 11:19 PM
Muestra1_Pos4.JPG	1.3 MB	1	0	2021-11-27 11:19 PM
Muestra1_Pos4_L.JPG	32.7 kB	1	0	2021-11-27 11:19 PM
Sample02				
Sample03				
Sample04				

Figure 4. Summary of file location.

4. User Notes

- These diagnostic images obtained with optical microscopy can be useful for researchers and data scientists working on computer-vision-based models for image segmentation and object detection using medical images. Recent studies have shown that the diagnosis of this disease from diagnostic imaging is a topic of worldwide interest [15,23], since the timely diagnosis of this disease can save many lives, especially immunocompromised patients.
- The presented dataset could be used to train, test, and validate computational models related to *Pneumocystis jirovecii* pneumonia diagnosis based on image analysis. For example, it is possible to use convolutional neural networks (CNNs) to address a binary classification of images obtained with optical microscopy. In this way, one of the most widely used diagnostic techniques for the detection of pneumonia can be improved.
- Our dataset includes annotations made by an expert in the diagnosis of *Pneumocystis jirovecii* pneumonia, which can be used to develop algorithms based on deep learning

that help to have a more automated diagnosis of this disease from images obtained with optical microscopy.

- The dataset reported in this work can be further segmented and processed in different free tools such as ImageJ, U-Net, ML-powered, OpenCV, and others. Furthermore, commercial software such as Matlab or Mathematica can be used for segmentation and further analysis.
- This is the first dataset based on medical images obtained with optical microscopy for analyzing whether a patient has *Pneumocystis jirovecii* pneumonia.

Author Contributions: E.R.-V.: conceptualization, methodology, visualization, investigation, software, data curation, formal analysis, and writing—original draft. J.S.B.-V.: investigation, software, data curation, formal analysis, and writing—original draft. K.A.-B.: methodology, resources, investigation, validation, and writing—original draft. A.Z.: supervision, writing—review and editing. T.W.N.: resources, supervision, writing—review and editing, and project administration. All authors have read and agreed to the published version of the manuscript.

Funding: Research reported in this publication was supported by Corporación Para Investigaciones Biológicas. Erick Reyes-Vera and J. Botero-Valencia acknowledges the support of Instituto Tecnológico Metropolitano through project P21101. The APC was funded by Corporación Para Investigaciones Biológicas, Instituto Tecnológico Metropolitano, and Universidad Pontificia Bolivariana.

Institutional Review Board Statement: Not applicable.

Informed Consent Statement: Not applicable.

Data Availability Statement: Data regarding images and annotations can be accessed at repository name: Microscopic imaging and labeling dataset for the detection of *Pneumocystis jirovecii* using methenamine silver staining method (DOI 10.17605/OSF.IO/WQME8); direct URL to data: <https://osf.io/96r3h/> (accessed on 15 February 2022).

Conflicts of Interest: The authors declare no conflict of interest.

References

1. Vielle Peggy, F.D. Métodos Diagnósticos Tintoriales para *Pneumocystis jirovecii* (Diagnostic methods staining for *Pneumocystis jirovecii*). *Boletín Medico* **2011**, *26*, 29–34.
2. Saraiva, A.A.; Santos, D.B.; Costa, N.C.; Sousa, J.V.M.; Fonseca Ferreira, N.M.; Valente, A.; Soares, S. Models of Learning to Classify X-ray Images for the Detection of Pneumonia using Neural Networks. In Proceedings of the 12th International Joint Conference on Biomedical Engineering Systems and Technologies—BIOIMAGING, Prague, Czech Republic, 22–24 February 2019; Volume 1, pp. 76–83. [\[CrossRef\]](#)
3. Hammarström, H.; Grankvist, A.; Broman, I.; Kondori, N.; Wennerås, C.; Gisslen, M.; Friman, V. Serum-based diagnosis of *Pneumocystis pneumonia* by detection of *Pneumocystis jirovecii* DNA and 1,3- β -D-glucan in HIV-infected patients: A retrospective case control study. *BMC Infect. Dis.* **2019**, *19*, 658. [\[CrossRef\]](#) [\[PubMed\]](#)
4. Clarkson, A.B.; Merali, S. *Pneumocystis pneumonia*, 1st ed.; CRC Press: Boca Raton, FL, USA, 2009; pp. 227–236. [\[CrossRef\]](#)
5. Kaur, R.; Wadhwa, A.; Bhalla, P.; Dhakad, M.S. *Pneumocystis pneumonia* in HIV patients: A diagnostic challenge till date. *Med. Mycol.* **2015**, *53*, 587–592. [\[CrossRef\]](#) [\[PubMed\]](#)
6. Song, Y.; Ren, Y.; Wang, X.; Li, R. Recent advances in the diagnosis of *Pneumocystis pneumonia*. *Med. Mycol. J.* **2016**, *57*, E111–E116. [\[CrossRef\]](#)
7. Baltazar, L.R.; Manzanillo, M.G.; Gaudillo, J.; Viray, E.D.; Domingo, M.; Tiangco, B.; Albia, J. Artificial intelligence on COVID-19 pneumonia detection using chest xray images. *PLoS ONE* **2021**, *16*, e0257884. [\[CrossRef\]](#)
8. Chumbita, M.; Cillóniz, C.; Puerta-Alcalde, P.; Moreno-García, E.; Sanjuan, G.; Garcia-Pouton, N.; Soriano, A.; Torres, A.; Garcia-Vidal, C. Can artificial intelligence improve the management of pneumonia. *J. Clin. Med.* **2020**, *9*, 248. [\[CrossRef\]](#)
9. Stokes, K.; Castaldo, R.; Federici, C.; Pagliara, S.; Maccaro, A.; Cappuccio, F.; Fico, G.; Salvatore, M.; Franzese, M.; Pecchia, L. The use of artificial intelligence systems in diagnosis of pneumonia via signs and symptoms: A systematic review. *Biomed. Signal Process. Control.* **2022**, *72*, 103325. [\[CrossRef\]](#)
10. Ebrahimian, S.; Homayounieh, F.; Rockenbach, M.A.; Putha, P.; Raj, T.; Dayan, I.; Bizzo, B.C.; Buch, V.; Wu, D.; Kim, K.; et al. Artificial intelligence matches subjective severity assessment of pneumonia for prediction of patient outcome and need for mechanical ventilation: A cohort study. *Sci. Rep.* **2021**, *11*, 858. [\[CrossRef\]](#)
11. Rodiño, J.; Rincón, N.; Aguilar, Y.A.; Rueda, Z.V.; Herrera, M.; Vélez, L.A. Diagnóstico microscópico de neumonía por *Pneumocystis jirovecii* en muestras de lavado broncoalveolar y lavado orofaríngeo de pacientes inmunocomprometidos con neumonía. *Biomédica* **2011**, *31*, 222. [\[CrossRef\]](#)

12. Alshahrani, M.Y.; Alfaifi, M.; Ahmad, I.; Alkhathami, A.G.; Hakami, A.R.; Ahmad, H.; Alshehri, O.M.; Dhakad, M.S. *Pneumocystis jirovecii* detection and comparison of multiple diagnostic methods with quantitative real-time PCR in patients with respiratory symptoms. *Saudi J. Biol. Sci.* **2020**, *27*, 1423–1427. [[CrossRef](#)]
13. Zhu, H.; Isikman, S.O.; Mudanyali, O.; Greenbaum, A.; Ozcan, A. Optical imaging Techniques for Point-Of-Care Diagnostics. *Lab Chip* **2013**, *13*, 51–67. [[CrossRef](#)] [[PubMed](#)]
14. Alanio, A.; Bretagne, S. Diagnosis of *Pneumocystis jirovecii* Pneumonia: Role of β -D-Glucan Detection and PCR. *Curr. Fungal Infect. Rep.* **2014**, *8*, 322–330. [[CrossRef](#)]
15. Jaiswal, A.K.; Tiwari, P.; Kumar, S.; Gupta, D.; Khanna, A.; Rodrigues, J.J. Identifying pneumonia in chest X-rays: A deep learning approach. *Measurement* **2019**, *145*, 511–518. [[CrossRef](#)]
16. Botero-Valencia, J.S.; Valencia-Aguirre, J. Portable low-cost IoT hyperspectral acquisition device for indoor/outdoor applications. *HardwareX* **2021**, *10*, e00216. [[CrossRef](#)]
17. Momenzadeh, M.; Sehhati, M.; Mehri Dehnavi, A.; Talebi, A.; Rabbani, H. Automatic diagnosis of vulvovaginal candidiasis from Pap smear images. *J. Microsc.* **2017**, *267*, 299–308. [[CrossRef](#)]
18. Asefpour Vakilian, K.; Massah, J. An artificial neural network approach to identify fungal diseases of cucumber (*Cucumis sativus* L.) plants using digital image processing. *Arch. Phytopathol. Plant Prot.* **2013**, *46*, 1580–1588. [[CrossRef](#)]
19. Ziyade, P.; Ahmadi, V.F.; Bazayr, P.; Cavallo, E. Comparison of different image processing methods for segregation of peanut (*Arachis hypogaea* L.) seeds infected by aflatoxin-producing fungi. *Agronomy* **2021**, *11*, 873. [[CrossRef](#)]
20. Tahir, M.W.; Zaidi, N.A.; Rao, A.A.; Blank, R.; Vellekoop, M.J.; Lang, W. A fungus spores dataset and a convolutional neural network based approach for fungus detection. *IEEE Trans. Nanobiosci.* **2018**, *17*, 281–290. [[CrossRef](#)]
21. Mäder, U.; Quiskamp, N.; Wildenhain, S.; Schmidts, T.; Mayser, P.; Runkel, F.; Fiebig, M. Image-Processing Scheme to Detect Superficial Fungal Infections of the Skin. *Comput. Math. Methods Med.* **2015**, *2015*, 851014. [[CrossRef](#)]
22. Sirazitdinov, I.; Kholiavchenko, M.; Mustafaev, T.; Yixuan, Y.; Kuleev, R.; Ibragimov, B. Deep neural network ensemble for pneumonia localization from a large-scale chest X-ray database. *Comput. Electr. Eng.* **2019**, *78*, 388–399. [[CrossRef](#)]
23. Kassania, S.H.; Kassanib, P.H.; Wesolowskic, M.J.; Schneidera, K.A.; Detersa, R. Automatic Detection of Coronavirus Disease (COVID-19) in X-ray and CT Images: A Machine Learning Based Approach. *Biocybern. Biomed. Eng.* **2021**, *41*, 867–879. [[CrossRef](#)] [[PubMed](#)]
24. Pujari, J.D.; Yakkundimath, R.; Byadgi, A.S. Image processing Based Detection of Fungal Diseases in Plants. *Procedia Comput. Sci.* **2015**, *46*, 1802–1808. [[CrossRef](#)]
25. Urda-Benitez, R.D.; Castro-Ospina, A.E.; Orozco-Duque, A. Feature extraction based on time-singularity multifractal spectrum distribution in intracardiac atrial fibrillation signals. *TecnoLógicas* **2017**, *20*, 97–111. [[CrossRef](#)]
26. Bedoya-Vargas, M.E.; Vásquez-Correa, J.C.; Orozco-Arroyave, J.R. Time-frequency representations from inertial sensors to characterize the gait in Parkinson's disease. *TecnoLógicas* **2018**, *21*, 53–69. [[CrossRef](#)]
27. Arteaga, M.A.; Castaneda, E. *Micosis Humanas, Procedimientos Diagnósticos—Exámenes directos*, 2nd ed.; Corporación para Investigaciones Biológicas: Medellín, Colombia, 2003; pp. 146–168.
28. Nassar, A.; Zapata, M.; Little, J.V.; Siddiqui, M.T. Utility of reflex gomori methenamine silver staining for *Pneumocystis jirovecii* on bronchoalveolar lavage cytologic specimens: A review. *Diagn. Cytopathol.* **2006**, *34*, 719–723. [[CrossRef](#)] [[PubMed](#)]
29. Reiss, E.; Shadomy, H.J.; Lyon, G.M., III. *Laboratory Diagnostic Methods in Medical Mycology*; John Wiley & Sons, Inc.: Hoboken, NJ, USA, 2011; pp. 31–73. [[CrossRef](#)]
30. Zuluaga, A.; Gonzalez, D.; Rua, A. *Diagnostico Micologico por el Laboratorio II: Examen Directo, Coloraciones y Medios de Cultivo*, 1st ed.; Corporacion para Investigaciones Biologicas: Medellín, Colombia, 2018; pp. 553–592.